Atomic Surface Structure for Unraveling the Trade-off between the Propane Dehydrogenation Activity and Anti-Deactivation of PtSn Catalysts

Mingxin Lv[1], Qiang Li[1*], Fan Xue[1], Zhiguo Li[1], Peixi Zhang[1], Yue Zhu[1], Longlong Fan[2], Jianrong Zeng[3], Qiheng Li[1], Xin Chen[1], Kun Lin[1], Jinxia Deng[1], Xianran Xing[1*]

[1] Institute of Solid State Chemistry, University of Science and Technology Beijing, Beijing Advanced Innovation Center for Materials Genome Engineering, Beijing 100083, China.

[2]Institute of High Energy Physics, CAS, Beijing100049, China.

[3]Shanghai Synchrotron Radiation Facility, Shanghai Advanced Research Institute, Chinese Academy of Sciences, Shanghai 201204; Shanghai Institute of Applied Physics, Chinese Academy of Sciences, Shanghai 201800, China.

1 Catalyst Preparation

PtSn bimetallic catalysts were synthesized by stepwise impregnation method, 7.71, 23.14, 38.56, 57.85mg $SnCl_2 \cdot 2H_2O$ were dissolved in 2.0 mL of methanol and added dropwise to 1g silica, the obtained Sn/SiO_2 were dried overnight at 80 °C and annealing at 450℃ for 4 hours, $H_2PtCl_6 \cdot 6H_2O$ was dissolved in 2.0 mL of water (45.66mg), then the solution was added dropwise to the obtained Sn/SiO_2. After the catalysts dried overnight at 80°C it was annealing at 250℃ for 4 hours, and aged at room temperature for two week. The silica supported was calcined in air at 500°C for 4 hours and cooled to room temperature. The aged catalysts were used for catalytic testing and characterization after pretreatment as described below.

2 Characterization

The powder X-ray diffraction (XRD) patterns of the catalysts were measured on a Rigaku SmartLab diffractometer using Cu Kα radiation (λ=1.54 Å, 40 kV and 30 mA), the scanning angle is 30 ~ 80° with 2°/min of scanning speed. X-ray photoelectron spectra were measured on Thermo Scientific K-Alpha with Al Kα radiation. Charge correction was used with C 1s orbital binding energy(284.8 eV) and Pt 4f spectra were analyzed by using XPSPEAK software. The morphology and size of PtSn nanoparticles were obtained on Titan ETEM G2 microscope operated at 300 kV. The high-angle annular dark-field scanning transmission electron microscopy (HAADF-STEM) images and energy-dispersive X-ray spectroscopy (EDS) analyses were obtained from an atomic-resolution analytical microscope (JEM-ARM 200F) with an operating voltage of 200 kV. The actual loadings of Pt and Sn are obtained by inductively coupled plasma optical emission spectroscopy (Agilent ICPOES 730).

A Bruker Tensor 27 instrument with a highly sensitive MCT detector and a diffuse IR heating chamber was utilized to record in situ diffuse reflectance Infrared Fourier transform spectroscopy (DRIFTS) of CO chemisorption over different PtSn nanocatalysts at room temperature. Prior to CO chemisorption, the catalysts were pretreated by H_2 at 250 °C for 30 min and then cooled down to room temperature in N_2, followed by the recording of a background at a resolution of 4 cm^{-1} with 256 scans. Then the catalysts were exposed to a CO flow for 30 min and purged with N_2 before

collecting the spectra.

Thermal gravimetric analysis (TG) were measured on PerKinElmer STA 8000, sample was heated in a flux of N_2 (20ml/min), the temperature range is 100-700°C, the heating rate is 10°C/min.

CO Pulse chemisorption were measured on Micromeritics AutoChem II 2920，Prior to CO chemisorption, the catalysts were pretreated by H_2 at 250 °C for 60 min. CO adsorption isotherms were collected at 35 °C . The dispersion was measured from the total adsorption isotherm, and the particle sizes were calculated using the inverse of the dispersion, assuming hemispherical shaped nanoparticles.

XAFS spectra were collected on the BL13SSW beamline of Shanghai Synchrotron Radiation Facility. Spectra were collected at the Pt L_3-edge, data was acquired in transmission mode at room temperature, using Demeter package to fit data[1]. Wavelet transform (WT) of Pt L_3-edge EXAFS was implemented by using the HAMA software[2].

Atomic pair distribution function (PDF) was obtained from 3W1 beamline at Beijing Synchrotron Radiation Facility with the wavelength of 0.2061 Å, the atomic pair distribution function (PDF) was obtained by direct Fourier transform of reduced structure function with a Q value of 20 $Å^{-1}$ by PDFgetX2 software[3]. Small box fitting was carried out on PDFgui based on Pt_3Sn, PtSn phase. RMCprofile was used to Reverse Monte Carlo for the PDF data in big box fitting[3], based on small box fitting unit cell , expanding this unit cells to a sphere with a radius of 15 Å and put it in a 50Å ×50Å × 50Å vacuum box generate the initial model of RMC[4]. DISCUS was uesd to analysis atomic spatial distribution and atom local coordination environment base model from RMC[4]. Pt-Pt coordination number was extracted by counting the number of Pt atoms in the 0-3.2Å range around Pt atoms.

RIR method with a powder specimen is as follows:

$$W_X = \frac{I_X}{K_A^X \times \sum_{i=A}^{N} \frac{I_i}{K_A^i}}$$

where W_x is the wt.% of the phase in the mixture, K_A is the RIR value and I_x is the

diffraction intensities.

3 Catalytic Activity Tests.

Catalyst PDH tests were carried out in fixed bed reactor with loading amount of 50mg. The catalyst was packed into a steel pipe with an inner diameter of 7.5 mm. Before the reaction, the catalyst was heated at 580 °C at a rate of 2 °C /min and pre-treated with 10%H_2/N_2 gas. The 10%H_2/N_2 gas flow rate was 50ml/min. Afterwards, the catalyst was evaluated at 580 °C and before each test, the catalyst was reduced at 580 °C for 60 min with 10%H_2/N_2 gas (100 mL/min). The gas composition of the reaction gas was C_3H_8: N_2=1:9, with a flow rate of 100ml/min and the reaction atmospheric pressure is 1atm. Long-term stability test for PDH conversion was evaluated at 550 °C, the reaction gas was C_3H_8:H_2:N_2=2:1:17(50 mL/min). The products were analyzed online by Techcomp GC7980 equipped with a flame ionization detector. the conversion and selectivity were calculated as follows:

$$Propane\ Conversion = \frac{n(C_3H_{8in}) - n(C_3H_{8out})}{n(C_3H_{8in})}$$

$$Propylene\ Selectivity = \frac{3 \times n(C_3H_6)}{n(CH_4) + 2 \times n(C_2H_6) + 2 \times n(C_2H_4) + 3 \times n(C_3H_6)}$$

$$Deactivation\ Rate = \frac{ln((1 - X_{final})/X_{final}) - ln((1 - X_{initial})/X_{initial})}{t}$$

Where $n(C_3H_{8in})$ and $n(C_3H_{8out})$ are the molar of propane in the feed/exit flow, $n(C_3H_6)$, $n(C_2H_4)$, $n(C_2H_6)$, $n(CH_4)$ are the molar of hydrocarbons in the exit flow, X_{final} is final conversion of propane, $X_{initial}$ is initial conversion of propane, t is reaction time.

4 Density Functional Theory (DFT) Calculations.

First principle calculations based on the projector augmented wave (PAW)[5] were performed using Vienna ab initio simulation package (VASP)[6]. Exchange–correlation functional of Perdew–Burke–Ernzerh within the generalized gradient approximation was adopted, the cut-off energy for the basis set was chose as 400 eV. The Brillouin zone was sampled using a 3×3×1k-mesh. The original surface models of the $Pt_{80}Sn_{20}$,$Pt_{53}Sn_{47}$ catalysts is six-layer atoms on the Pt_3Sn (1 1 1) surface, and

$Pt_{42}Sn_{58}$,$Pt_{33}Sn_{67}$ is on the PtSn (0 0 1) surface. By adjusting the distribution of the outermost and second outermost atoms, the model of central Pt sites on catalysts surface with 0, 3, 6, 9 Pt-Pt coordination numbers were acquired. The vacuum layer of was set as 15 Å.

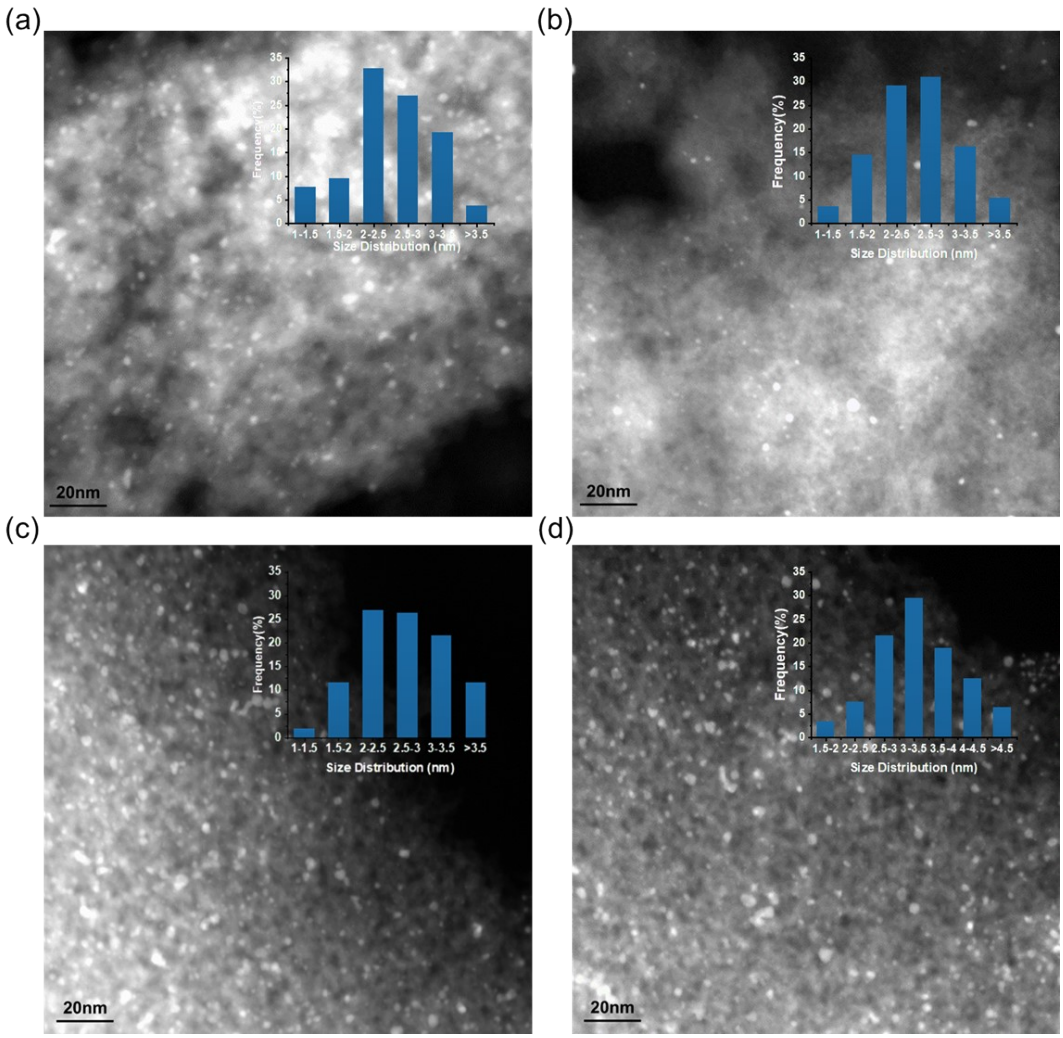

Figure S1. STEM image of PtSn catalysts. (a) $Pt_{80}Sn_{20}$, (b) $Pt_{53}Sn_{47}$, (c) $Pt_{42}Sn_{58}$, (d) $Pt_{33}Sn_{67}$.

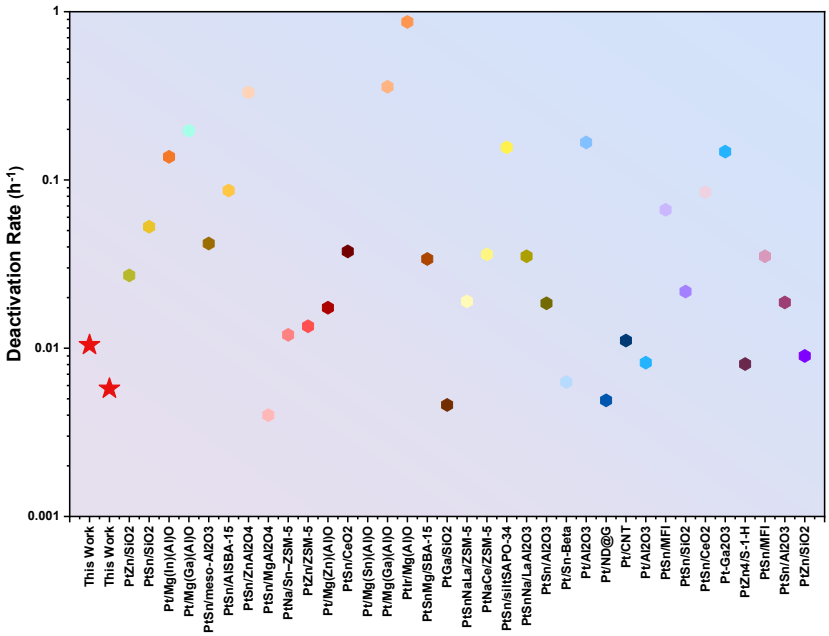

Figure S2. Deactivation rate of different Pt-base catalysts reported in the literature for propane dehydrogenation[7-41].

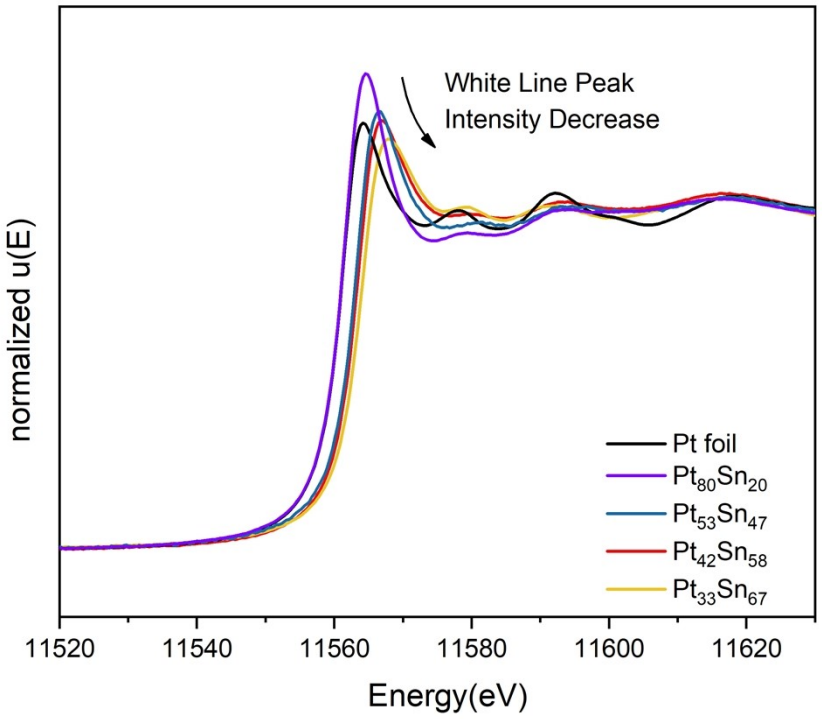

Figure S3. Normalized Pt L_3-edge XANES spectra of $Pt_{80}Sn_{20}$, $Pt_{53}Sn_{47}$, $Pt_{42}Sn_{58}$, $Pt_{33}Sn_{67}$ nanocatalysts.

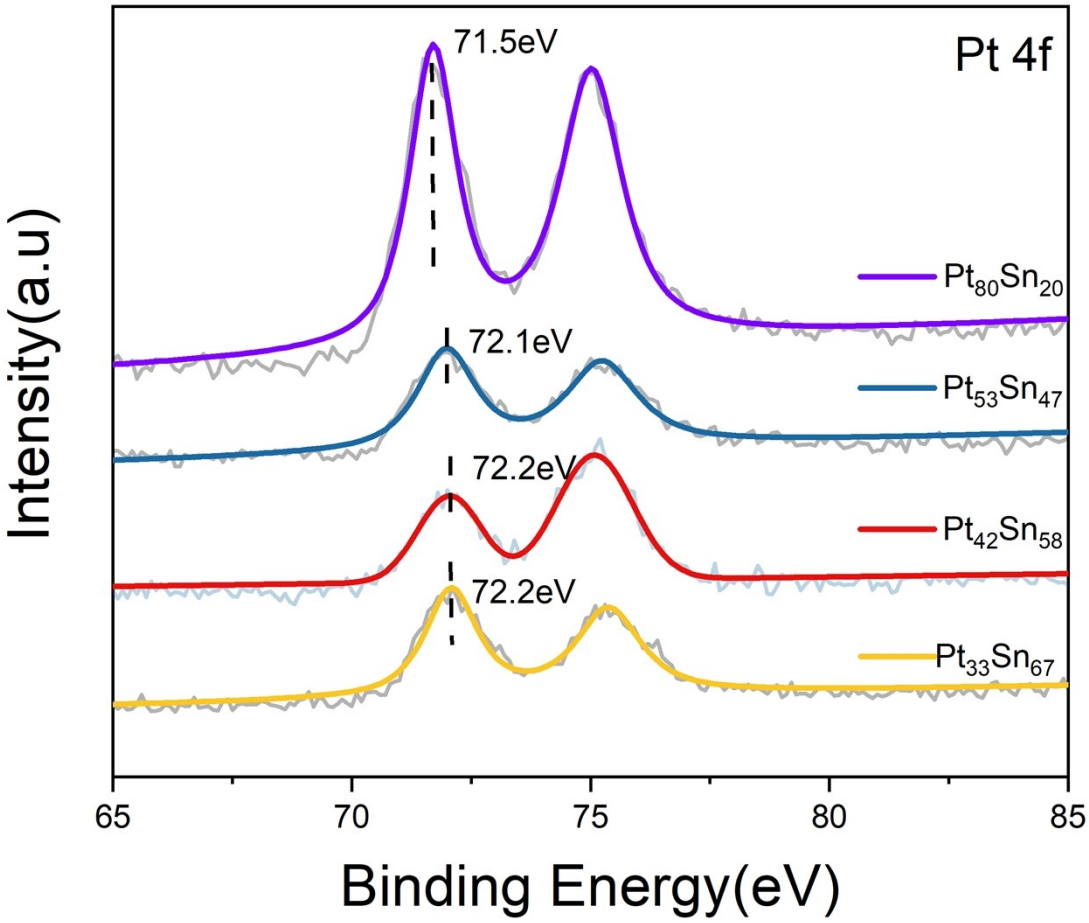

Figure S4. XPS spectra of $Pt_{80}Sn_{20}$, $Pt_{53}Sn_{47}$, $Pt_{42}Sn_{58}$, $Pt_{33}Sn_{67}$ nanocatalysts.

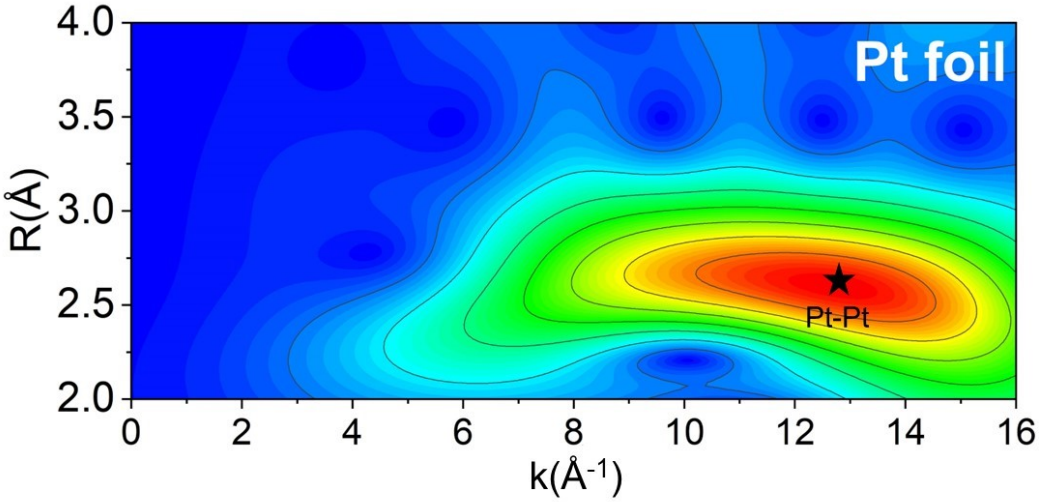

Figure S5. Wavelet transform of Pt foil Pt L_3-edge EXAFS in the R-space 2.0 to 4.0 Å

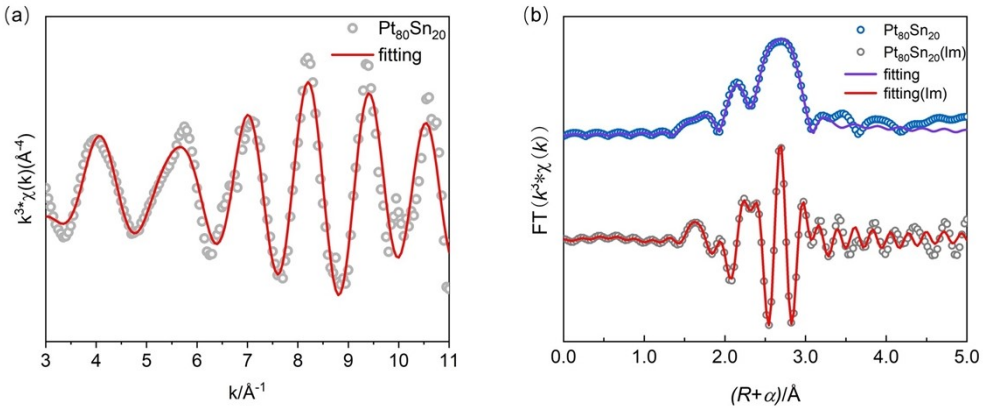

Figure S6 Fitting results of the EXAFS spectra of $Pt_{80}Sn_{20}$ catalysts. (FT range: 3.00 Å^{-1}–11.00 Å^{-1}, Fitting range: 2.00 Å–3.50 Å)

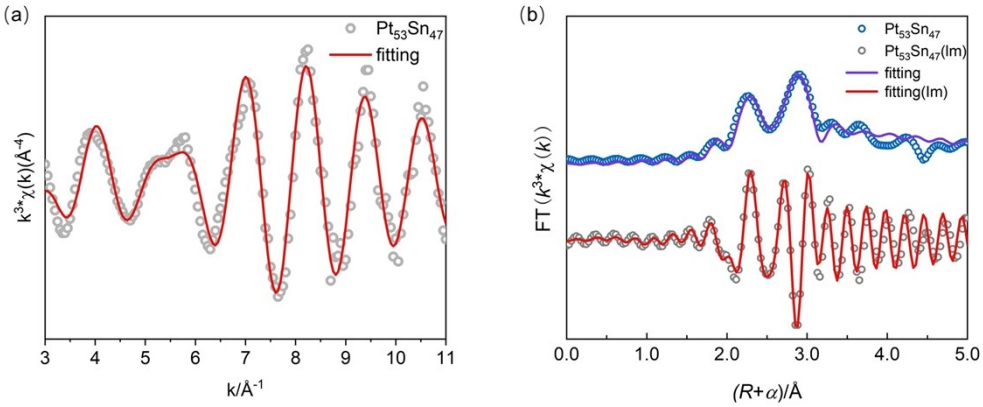

Figure S7 Fitting results of the EXAFS spectra of $Pt_{53}Sn_{47}$ catalysts. (FT range: 3.00 Å-1–11.00 Å-1, Fitting range: 2.00 Å–3.50 Å)

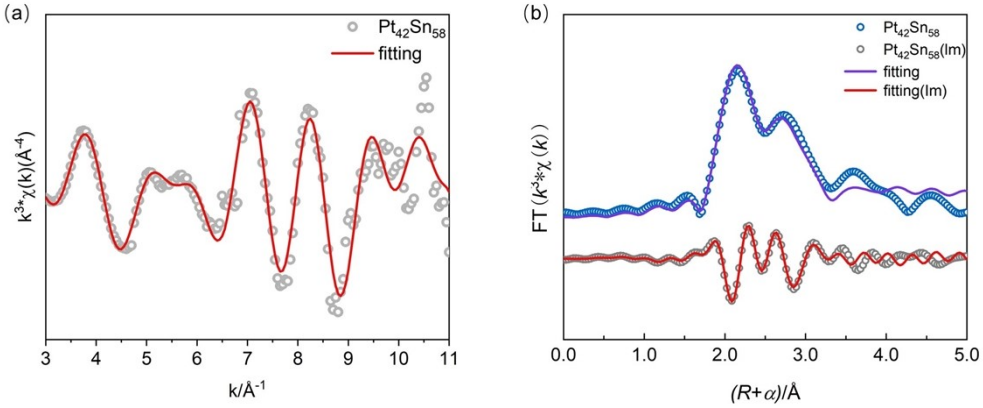

Figure S8 Fitting results of the EXAFS spectra of $Pt_{42}Sn_{58}$ catalysts. (FT range: 3.00 Å-1–11.00 Å-1, Fitting range: 2.00 Å–3.50 Å)

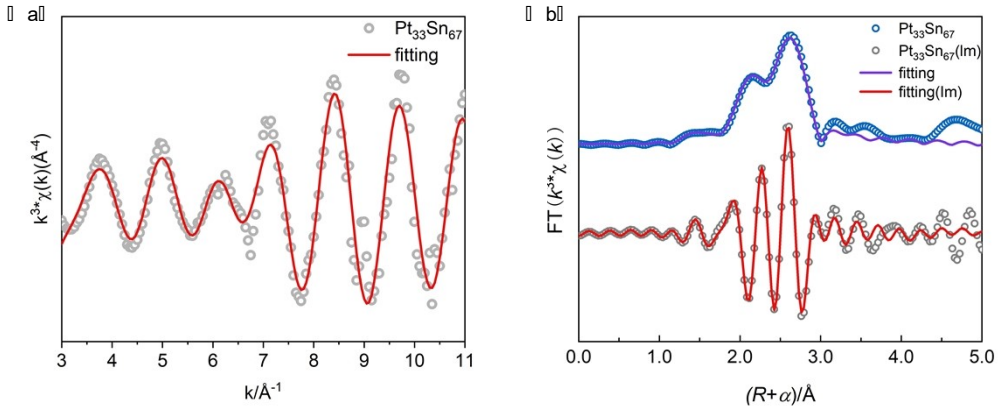

Figure S9 Fitting results of the EXAFS spectra of $Pt_{33}Sn_{67}$ catalysts. (FT range: 3.00 Å-1–11.00 Å-1, Fitting range: 2.00 Å–3.50 Å)

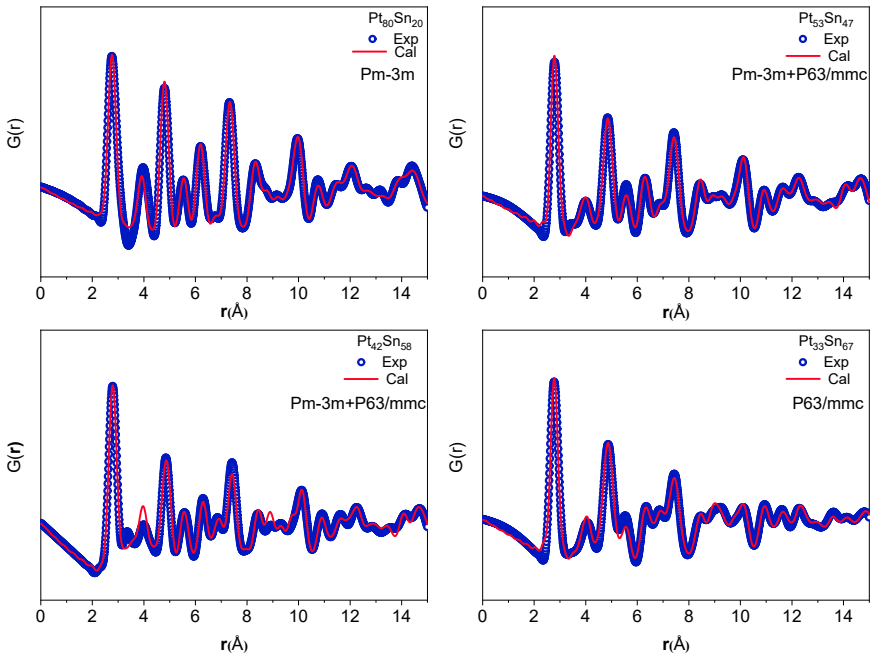

Figure S10. Atomic pair distribution functions and small-box fitting results of PtSn catalysts. (a) $Pt_{80}Sn_{20}$, (b) $Pt_{53}Sn_{47}$, (c) $Pt_{42}Sn_{58}$, (d) $Pt_{33}Sn_{67}$.

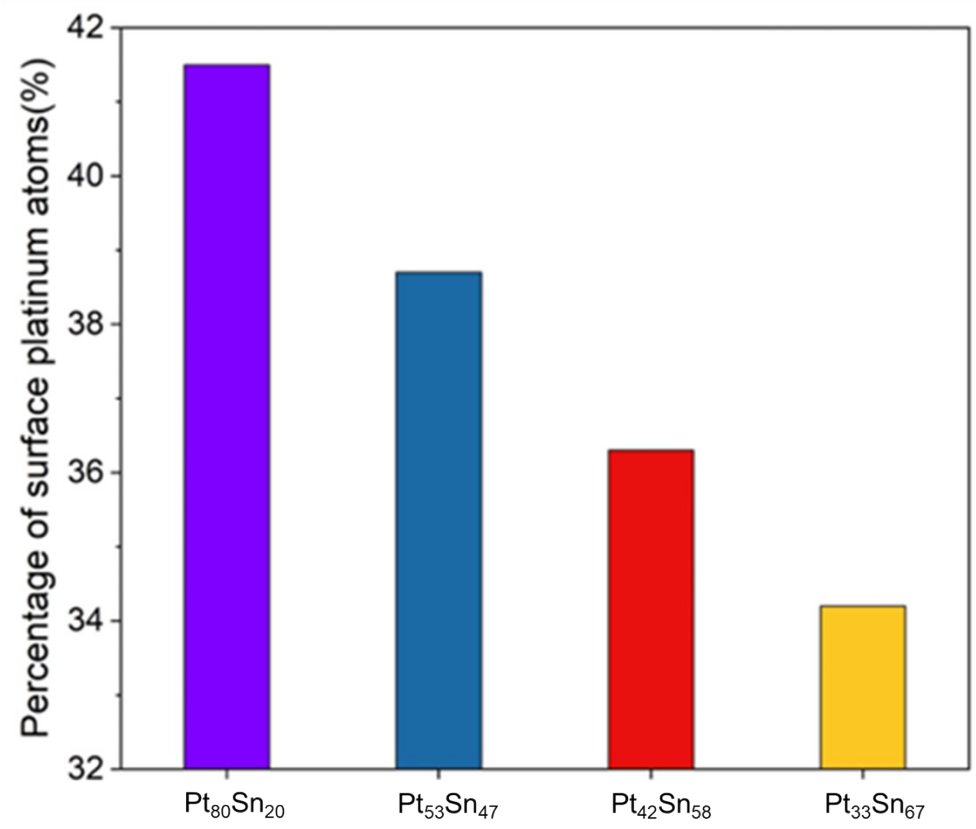

Figure S11. Proportion of surface platinum atoms among all platinum atoms (Extraction from the three-dimensional atomic distribution)

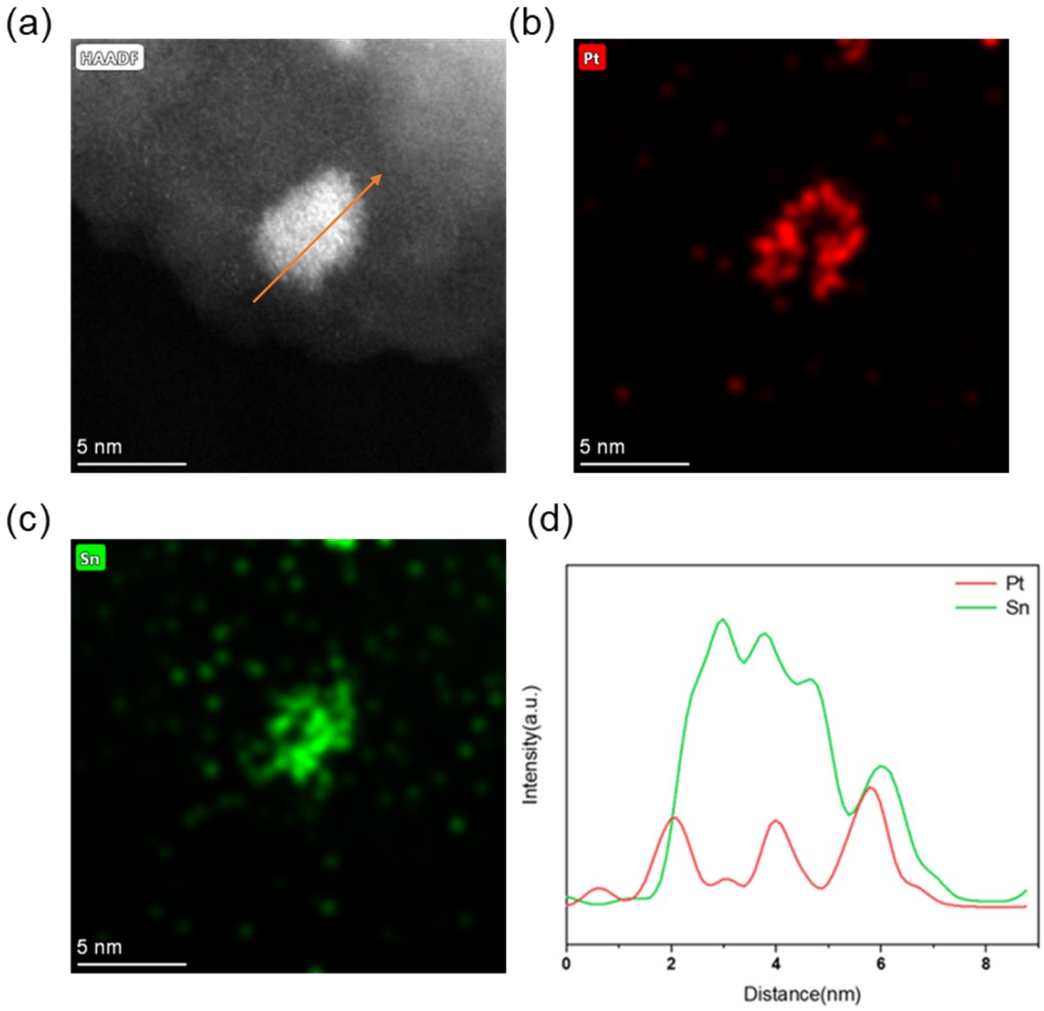

Figure S12. EDS elemental mapping and line-scanning profile of $Pt_{33}Sn_{67}$.

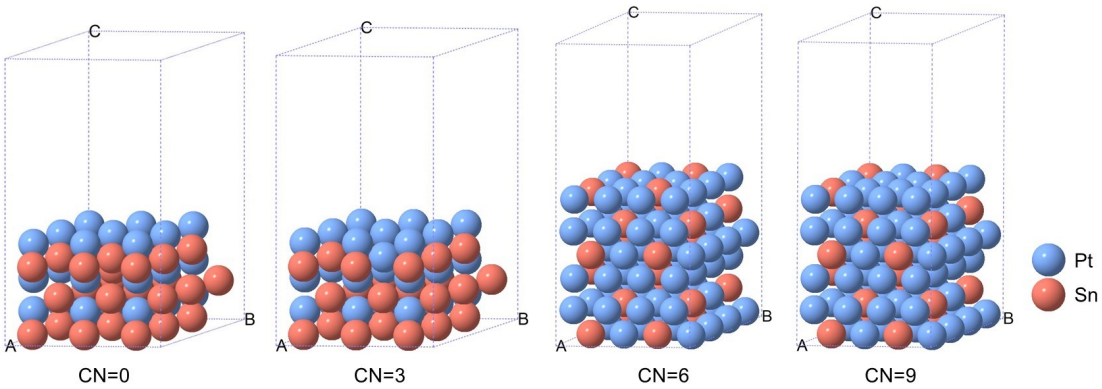

Figure S13 The constructed PtSn surface models with different Pt-Pt coordination numbers for DFT calculations.

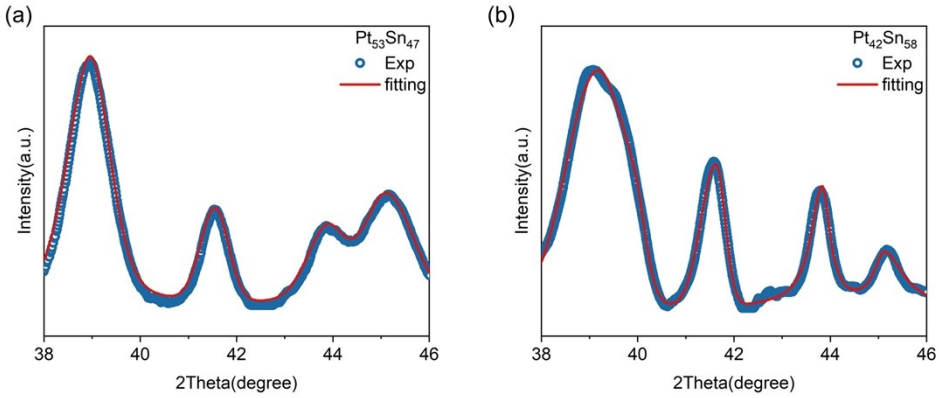

Figure S14 The strongest peaks of $Pt_{53}Sn_{47}$ and $Pt_{42}Sn_{58}$ were fitted using Jade to obtain peak shape parameters.

Table S1 Chemical compositions and elemental loading amounts of $PtSn/SiO_2$ samples determined by ICP-OES

Sample	Molar ratios of Pt:Sn	Loading amounts of Pt(wt%)	Loading amounts of Sn(wt%)
$Pt_{80}Sn_{20}$	80:20	1.68	0.26
$Pt_{53}Sn_{47}$	53:47	1.92	1.07
$Pt_{42}Sn_{58}$	42:58	1.71	1.46
$Pt_{33}Sn_{67}$	33:67	1.58	2.00

Table S2. Pt dispersion of PtSn catalysts

Sample	Pt dispersion%	Pt particle diameter/nm
$Pt_{80}Sn_{20}$	57.23	1.96
$Pt_{53}Sn_{47}$	57.42	1.95
$Pt_{42}Sn_{58}$	40.00	3.73
$Pt_{33}Sn_{67}$	29.04	4.75

Table S3 Average coordination number obtained from fitting results of Pt L_3-edge EXAFS data[a] and RMC

Sample	Path	ΔE_0(eV)	CN[b]	R/Å[b]	σ^2/ Å^2	R factor	CN[c]	R/Å[c]
$Pt_{80}Sn_{20}$	Pt-Pt	10.20	6.62±0.37	2.77±0.04	0.0078±0.001	0.003	7.35	2.80
	Pt-Sn	2.30	1.22±0.62	2.75±0.01	0.0158±0.004	0.003	1.52	2.82
$Pt_{53}Sn_{47}$	Pt-Pt	11.20	6.05±1.13	2.80±0.01	0.0110±0.002	0.007	5.20	2.82
	Pt-Sn	11.46	2.96±2.60	2.86±0.01	0.02337±0.018	0.007	3.21	2.86
$Pt_{42}Sn_{58}$	Pt-Pt	12.57	2.85±0.45	2.82±0.01	0.0019±0.0010	0.003	3.36	2.78
	Pt-Sn	3.89	3.96±0.79	2.83±0.03	0.0179±0.0037	0.003	3.95	2.81
$Pt_{33}Sn_{67}$	Pt-Pt	11.50	2.31±0.74	2.81±0.07	0.0011±0.0068	0.006	2.61	2.79
	Pt-Sn	6.99	3.36±0.18	2.75±0.01	0.0049±0.0044	0.006	3.63	2.78

[a] $S0_2$ was fix as 0.795 which is obtained from the fitting for Pt-foil. Data ranges: 3.0≤K≤11.00 Å^{-1}, 2.0≤R≤3.5 Å. Fitting was performed in q-space with k^3 weighting.

[b] Extract through fitting of EXAFS.

[c] Extract through discussion from RMC result.

Table S4 Fitting results of PDF data for PtSn catalysts with PDFgui

Sample	Phase	Phase ratio	a/Å[a]	b/Å[a]	c/Å[a]
$Pt_{80}Sn_{20}$	Pt_3Sn	-	3.9824	3.9824	3.9824
$Pt_{53}Sn_{47}$	Pt_3Sn	71%	3.9807	3.9807	3.9807
	Pt_1Sn_1	29%	4.1755	4.1755	5.4777
$Pt_{42}Sn_{58}$	Pt_3Sn	49%	3.9872	3.9872	3.9872
	Pt_1Sn_1	51%	4.1637	4.1637	5.4658
$Pt_{33}Sn_{67}$	Pt_1Sn_1	-	4.1340	4.1340	5.4556

[a] lattice parameter

Table S5 Quantitative results of RIR method

Sample	phase	2-Theta	plane	Area	I%	RiR	w%	mol%
$Pt_{53}Sn_{47}$	Pt3Sn	38.97	(111)	150666	100	22.79	79.1	62.8
	PtSn	41.55	(102)	23341	15.5	13.23	20.9	37.2
$Pt_{42}Sn_{58}$	Pt3Sn	38.92	(111)	58125	100	22.79	68.2	48.8
	PtSn	41.54	(102)	15767	27.1	13.23	31.8	51.2

Table S6 Summary of the catalytic data of Pt-based dehydrogenation catalysts

#	Catalyst	Temp./ ℃	WHSV/ h^{-1}	Components /vol./%	Initial conversion/%	Selectivity /%	k_d^c /h^{-1}	Ref.
1	$PtSn/SiO_2$	580	5.9	10%C_3H_8 90%N_2	44.3	99.3	0.0057	This work
2	$PtSn/SiO_2$	580	5.9	10%C_3H_8 90%N_2	51.8	98.5	0.0104	This work
3	PtSn/meso-Al_2O_3	590	3.0	80%C_3H_8 20%He	30	92	0.0419	11
4	PtSn/AlSBA-15	590	3.0	80%C_3H_8 20%He	28	94.5	0.0866	12
5	$PtSn/ZnAl_2O_4$	600	8.8	23%C_3H_8 77%N_2	50	98	0.3312	13
6	$PtSn/MgAl_2O_4$	580	2.2	10%C_3H_8 10%H_2 80%He	46.4	96	0.004	14
7	PtNa/Sn–ZSM-5	590	3.0	80%C_3H_8 20%H_2	41.7	93	0.012	15
8	PtZn/ZSM-5	590	3.0	80%C_3H_8 20%H_2	40.6	96	0.0135	16
9	Pt/Mg(Zn)(Al)O	550	8.0	80%C_3H_8 20%H_2	20	99.3	0.0174	17
10	$PtSn/CeO_2$	680	2.2	16.7%C_3H_8 83.3%He	45	98	0.0376	18
11	Pt/Mg(Sn)(Al)O	550	14	29%C_3H_8 14%H_2 57%Ar	29.5	95	4E-4	19
12	Pt/Mg(Ga)(Al)O	600	26	20%C_3H_8 80%N_2	13.5	98	0.3576	20
13	PtIr/Mg(Al)O	600	51.9	80%C_3H_8 20%H_2	24.7	88	0.8695	21
14	PtSnMg/SBA-15	580	8.3	70%C_3H_8 30%Ar	43	97.8	0.0339	22
15	$PtGa/SiO_2$	550	9.8	20%C_3H_8 80%Ar	31.9	99	0.0046	23
16	PtSnNaLa/ZSM	590	3.0	80%C_3H_8 20%H_2	37.2	86.2	0.019	24
17	PtNaCe/ZSM-5	590	3.0	80%C_3H_8 20%H_2	42	92.6	0.0361	25
18	PtSn/siltSAPO	585	5.0	83%C_3H_8 17%H_2	38.2	79	0.1562	26

19	PtSnNa/$LaAl_2O_3$	590	3.0	80%C_3H_8 20%H_2	41	96.2	0.0352	27
20	PtSn/Al_2O_3	590	5.2	16%C_3H_8 20%H_2 64%He	49	97	0.0185	28
21	Pt/Al_2O_3	550	4，0	80%C_3H_8 20%H_2	33	35	0.1671	30
22	Pt/ND@G	600	1.6	5%C_3H_8 95%N_2	16.4	88	0.0049	31
23	Pt/CNT	600	1.6	5%C_3H_8 95%Ar	10.4	75	0.0111	32
24	Pt/Al_2O_3	590	9.4	16%C_3H_8 20%H_2 64%Ar	48.7	98	0.0082	33
25	PtSn/CeO_2	680	2.2	16.7%C_3H_8 83.3%He	45	78.0	0.0845	36
26	Pt-Ga_2O_3	620	5.4	20%C_3H_8 80%He	58.5	98	0.1473	37
27	PtSn/MFI	450	1.7	24%C_3H_8 76%He	70	90	0.0352	39
28	PtSn/SiO_2	580	4.7	16%C_3H_8 84%He	62	99	0.0087	40
29	PtZn/SiO_2	550	4.0	16%C_3H_8 16%H_2 68%N_2	58.9	99	0.009	41
30	PtSn/SiO_2	550	3.9	2%C_3H_8 5%H_2 93%N_2	11.2	99	0.0652	42
31	Pt-Ge-d4r@UTL	580	4.8	100%C_3H_8	45	95	0.0363	43
32	SiPtGa/Al_2O_3	450	0.59	2.5%C_3H_8 2.5%H_2 95%N_2	22	90	0.007	44
33	PtZnSn/	500	0.15	5%C_3H_8 95%N_2	47.6	99	0.0275	45

5 References

(1) Ravel, B, Newville, M., ATHENA, ARTEMIS, HEPHAESTUS: data analysis for X-ray absorption spectroscopy using IFEFFIT. *Journal of synchrotron radiation* **2005**, 12, 537-541.

(2) Funke, H, Scheinost, A. C, Chukalina, M. Wavelet analysis of extended x-ray absorption fine structure data *Phys. Rev. B* **2005**, 71, 94110-1-7.

(3) Qiu, X, Thompson, J. W, Billinge, S. J., PDFgetX2: a GUI-driven program to obtain the pair distribution function from X-ray powder diffraction data. *J. Appl. Crystallogr* 2004, 37, 678-678.

(4) Tucker, M, Dove, M, Goodwin, A, Keen, D, Playford, H, Slawinski, W. A., RMCProfile User Manual. *Code version* **2014**, 6, 0-155.

(5) Kresse, G.; Furthmüller, J. Efficiency of ab-initio total energy calculations for metals and semiconductors using a plane-wave basis set. Comput. Mater. Sci.**1996**, 6, 15−50.

(6) Blöchl, P. E. Projector augmented-wave method. Phys. Rev. B **1994**, 50, 17953.

(7) Rochlitz, L, Searles, K, Alfke, J, Zemlyanov, D, Safonova, O. V, Copéret, C., Silica-supported, narrowly distributed, subnanometric Pt–Zn particles from single sites with high propane dehydrogenation performance. *Chem. Sci.* **2020**, 11, 1549-1555.

(8) Deng, L, Miura, H, Shishido, T, Wang, Z, Hosokawa, S, Teramura, K, Tanaka, T., Elucidating strong metal-support interactions in Pt–Sn/SiO_2 catalyst and its consequences for dehydrogenation of lower alkanes. *J.Catal.* **2018**, 365, 277-291.

(9) Sun, P, Siddiqi, G, Vining, W. C, Chi, M, Bell, A. T., Novel Pt/Mg (In)(Al) O catalysts for ethane and propane dehydrogenation. *J. Catal.* **2011**, 282, 165-174.

(10) Zhu, Y, An, Z, Song, H, Xiang, X, Yan, W, He, J., Lattice-Confined Sn (IV/II) Stabilizing Raft-Like Pt Clusters: High Selectivity and Durability in Propane Dehydrogenation. *ACS Catal.* **2017**, **7**, 6973-6978.

(11) Motagamwala, A. H, Almallahi, R, Wortman, J, Igenegbai, V. O, Linic, S., Stable and selective catalysts for propane dehydrogenation operating at thermodynamic limit. *Science* **2021**, 373, 217-222.

(12) Jang, E. J, Lee, J, Jeong, H. Y, Kwak, J. H., Controlling the acid-base properties of alumina for stable PtSn-based propane dehydrogenation catalysts. *Appl. Catal. A.* **2019**, 572, 1-8.

(13) Redekop, E. A, Galvita, V. V, Poelman, H, Bliznuk, V, Detavernier, C, Marin, G. B., Delivering a Modifying Element to Metal Nanoparticles via Support: Pt–Ga Alloying during the Reduction of Pt/Mg(Al, Ga)O_x Catalysts and Its Effects on Propane Dehydrogenation. *ACS Catal.* **2014**, 4, 1812-1824.

(14) Li, J, Li, J, Zhao, Z, Fan, X, Liu, J, Wei, Y, Duan, A, Xie, Z, Liu, Q., Size effect of TS-1 supports on the catalytic performance of PtSn/TS-1 catalysts for propane dehydrogenation. *J. Catal.* **2017**, 352, 361-370.

(15) Zhang, H, Wan, H, Zhao, Y, Wang, W., Effect of chlorine elimination from Pt-Sn catalyst on the behavior of hydrocarbon reconstruction in propane dehydrogenation. *Catal. Today* **2019**, 330, 85-91.

(16) Wang, P, Yao, J, Jiang, Q, Gao, X, Lin, D, Yang, H, Wu, L, Tang, Y, Tan, L., Stabilizing the isolated Pt sites on PtGa/Al_2O_3 catalyst via silica coating layers for propane dehydrogenation at low temperature. *Appl. Catal. B* **2022**, 300.

(17) Zhu, H, Anjum, D. H, Wang, Q, Abou-Hamad, E, Emsley, L, Dong, H, Laveille, P, Li, L, Samal, A. K, Basset, J.-M., Sn surface-enriched Pt–Sn bimetallic nanoparticles as a selective and stable catalyst for propane dehydrogenation. *Journal of Catalysis* **2014**, 320, 52-62.

(18) Liu, L, Lopez-Haro, M, Lopes, C. W, Li, C, Concepcion, P, Simonelli, L, Calvino, J. J, Corma, A., Regioselective generation and reactivity control of subnanometric platinum clusters in zeolites for high-temperature catalysis. *Nat. Mater.* **2019**, 18 (8), 866-873.

(19) Wan, H, Qian, L, Gong, N, Hou, H, Dou, X, Zheng, L, Zhang, L, Liu, L., Size-Dependent Structures and Catalytic Properties of Supported Bimetallic PtSn Catalysts for Propane Dehydrogenation Reaction. *ACS Catal.* **2023**, 13 (11), 7383-7394.

(20) Werghi, B, Wu, L, Ebrahim, A. M, Chi, M, Ni, H, Cargnello, M, Bare, S. R., Selective Catalytic Behavior Induced by Crystal-Phase Transformation in Well-Defined Bimetallic Pt-Sn Nanocrystals. *Small* **2023**, 19 (20), 2207956.

(21) Iglesias-Juez, A, Beale, A. M, Maaijen, K, Weng, T. C, Glatzel, P, Weckhuysen, B. M., A combined in situ time-resolved UV–Vis, Raman and high-energy resolution X-ray absorption spectroscopy study on the deactivation behavior of Pt and PtSn propane dehydrogenation catalysts under industrial reaction conditions. *J. Catal.* **2010**, 276 (2), 268-279.

(22) Shi, L, Deng, G. M, Li, W. C, Miao, S, Wang, Q. N, Zhang, W. P, Lu, A. H., Al2O3 Nanosheets Rich in Pentacoordinate Al3+ Ions Stabilize Pt-Sn Clusters for Propane Dehydrogenation. *Angew. Chem. Int. Ed.* **2015**, 54 (47), 13994-13998

(23) Zhu, J, Yang, M.-L, Yu, Y, Zhu, Y.-A, Sui, Z.-J, Zhou, X.-G, Holmen, A, Chen, D., Size-Dependent Reaction Mechanism and Kinetics for Propane Dehydrogenation over Pt Catalysts. *ACS Catalysis* **2015**, 5 (11), 6310-6319.

(24) Im, J, Choi, M., Physicochemical Stabilization of Pt against Sintering for a Dehydrogenation Catalyst with High Activity, Selectivity, and Durability. *ACS Catalysi*s **2016**, 6 (5), 2819-2826.

(25) Liu, J, Yue, Y, Liu, H, Da, Z, Liu, C, Ma, A, Rong, J, Su, D, Bao, X, Zheng, H., Origin of the Robust Catalytic Performance of Nanodiamond–Graphene-Supported Pt Nanoparticles Used in the Propane Dehydrogenation Reaction. *ACS Catal.* **2017**, 7 (5), 3349-3355

(26) Xiong, H, Lin, S, Goetze, J, Pletcher, P, Guo, H, Kovarik, L, Artyushkova, K, Weckhuysen, B. M, Datye, A. K., Thermally Stable and Regenerable Platinum-Tin Clusters for Propane Dehydrogenation Prepared by Atom Trapping on Ceria. *Angew. Chem. Int. Ed.* **2017**, 56 (31), 8986-8991.

(27) Searles, K, Chan, K. W, Mendes Burak, J. A, Zemlyanov, D, Safonova, O, Coperet, C., Highly Productive Propane Dehydrogenation Catalyst Using Silica-Supported Ga-Pt Nanoparticles Generated from Single-Sites. *J. Am. Chem. Soc.* **2018**, 140 (37), 11674-11679.

(28) Zhao, S, Xu, B, Yu, L, Fan, Y., Catalytic dehydrogenation of propane to propylene over highly active PtSnNa/γ-Al_2O_3 catalyst. *Chinese Chem. Lett.* **2018**, 29 (3), 475-478

(29) Nakaya, Y, Hirayama, J, Yamazoe, S, Shimizu, K. I, Furukawa, S., Single-atom Pt in intermetallics as an ultrastable and selective catalyst for propane dehydrogenation. *Nat. Commun.* **2020**, 11 (1), 2838.

(30) Sun, Q, Wang, N, Fan, Q, Zeng, L, Mayoral, A, Miao, S, Yang, R, Jiang, Z, Zhou, W, Zhang, J, Zhang, T, Xu, J, Zhang, P, Cheng, J, Yang, D. C, Jia, R, Li, L, Zhang, Q, Wang, Y, Terasaki, O, Yu, J., Subnanometer Bimetallic Platinum–Zinc Clusters in Zeolites for Propane Dehydrogenation. *Angew. Chem. Int. Ed.* **2020**, 59 (44), 19450-19459.

(31) Ye, C, Peng, M, Wang, Y, Zhang, N, Wang, D, Jiao, M, Miller, J. T., Surface Hexagonal Pt1Sn1 Intermetallic on Pt Nanoparticles for Selective Propane Dehydrogenation. *ACS Appl. Mater. Interfaces* **2020**, 12 (23), 25903-25909.

(32) Chen, S, Zhao, Z.-J, Mu, R, Chang, X, Luo, J, Purdy, S. C, Kropf, A. J, Sun, G, Pei, C, Miller, J. T, Zhou, X, Vovk, E, Yang, Y, Gong, J., Propane Dehydrogenation on Single-Site [$PtZn_4$] Intermetallic Catalysts. *Chem* **2021**, 7 (2), 387-405.

(33) Han, S. W, Park, H, Han, J, Kim, J.-C, Lee, J, Jo, C, Ryoo, R., PtZn Intermetallic Compound Nanoparticles in Mesoporous Zeolite Exhibiting High Catalyst Durability for Propane Dehydrogenation. ACS *Catal.* **2021**, 11 (15), 9233-9241.

(34) Nakaya, Y, Xing, F, Ham, H, Shimizu, K. i, Furukawa, S., Doubly Decorated Platinum–Gallium Intermetallics as Stable Catalysts for Propane Dehydrogenation. *Angew. Chem. Int. Ed.* **2021**, 60 (36), 19715-19719.

(35) Wang, J, Chang, X, Chen, S, Sun, G, Zhou, X, Vovk, E, Yang, Y, Deng, W, Zhao, Z.-J, Mu, R, Pei, C, Gong, J., On the Role of Sn Segregation of Pt-Sn Catalysts for Propane Dehydrogenation. *ACS Catal.* **2021**, 11 (8), 4401-4410

(36) Ma, S, Liu, Z.-P., Zeolite-confined subnanometric PtSn mimicking mortise-and-tenon joinery for catalytic propane dehydrogenation. *Nat. Commun.* **2022**, 13 (1).

(37) Ye, C, Peng, M, Li, Y, Wang, D, Chen, C, Li, Y., Atomically dispersed Pt in ordered PtSnZn intermetallic with Pt−Sn and Pt−Zn pairs for selective propane dehydrogenation. *Sci. China Mater.* **2022**, 66 (3), 1071-1078.

(38) Brack, E, Plodinec, M, Willinger, M.-G, Copéret, C., Implications of Ga promotion and metal–oxide interface from tailored PtGa propane dehydrogenation catalysts supported on carbon. *Chem. Sci.* **2023**, 14 (44), 12739-12746.

(39) Zhang, Y, Zhou, Y, Tang, M, Liu, X, Duan, Y., Effect of La calcination temperature on catalytic performance of PtSnNaLa/ZSM-5 catalyst for propane dehydrogenation. *Chem. Eng. J.* **2012**, 181, 530-537.

(40) Motagamwala, A. H.; Almallahi, R.; Wortman, J.; Igenegbai, V. O.; Linic, S., Stable and selective catalysts for propane dehydrogenation operating at thermodynamic limit. Science 2021, 373 (6551), 217-222.

(41) Wei, P, Chen, S, Luo, R, Sun, G, Wu, K, Fu, D, Gong, J., Stable and homogeneous intermetallic alloys by atomic gas-migration for propane dehydrogenation. Nature Commun. **2024**,15(1), 8157.

(42) Ye, C.; Peng, M.; Wang, Y.; Zhang, N.; Wang, D.; Jiao, M.; Miller, J. T., Surface Hexagonal Pt1Sn1 Intermetallic on Pt Nanoparticles for Selective Propane Dehydrogenation. ACS Appl. Mater. Interfaces **2020**, 12 (23), 25903-25909.

(43) Ma, Y.; Song, S.; Liu, C.; Liu, L.; Zhang, L.; Zhao, Y.; Wang, X.; Xu, H.; Guan, Y.; Jiang, J., Germanium-enriched double-four-membered-ring units inducing zeolite-confined subnanometric Pt clusters for efficient propane dehydrogenation. Nat. Catal. **2023**, 6 (6), 506-518.

(44) Wang, P.; Yao, J.; Jiang, Q.; Gao, X.; Lin, D.; Yang, H.; Wu, L.; Tang, Y.; Tan, L., Stabilizing the isolated Pt sites on PtGa/Al2O3 catalyst via silica coating layers for propane dehydrogenation at low temperature. Appl. Catal. B: Environ. **2022**, 300, 120731.

(45) 1. Ye, C.; Peng, M.; Li, Y.; Wang, D.; Chen, C.; Li, Y., Atomically dispersed Pt in ordered PtSnZn intermetallic with Pt− Sn and Pt− Zn pairs for selective propane dehydrogenation. Sci. China Mater. **2023**, 66 (3), 1071-1078.